Am J Transl Res 2025;17(2):818-831
www.ajtr.org /ISSN:1943-8141/AJTR0161198

Original Article

Accuracy of 3D CE-MRA combined with ultrasound microbubble angiography for the diagnosis of lower extremity atherosclerotic occlusion

Junzhi Sang[1], Chunyu Zhang[1], Luting Lv[2], Ying Wang[3], Tianren Zhao[1], Xuena E[1]

[1]The Medical Imaging Center, The Second Affiliated Hospital of Qiqihar Medical University, Qiqihar 161006, Heilongjiang, China; [2]Department of Neurology, The Second Affiliated Hospital of Qiqihar Medical University, Qiqihar 161006, Heilongjiang, China; [3]Derpartment of Vascular Surgery, The Second Affiliated Hospital of Qiqihar Medical University, Qiqihar 161006, Heilongjiang, China

Received October 15, 2024; Accepted January 2, 2025; Epub February 15, 2025; Published February 28, 2025

Abstract: Objectives: To evaluate the diagnostic performance of 3D contrast-enhanced magnetic resonance angiography (3D CE-MRA) and ultrasound microbubble angiography, individually and combined, using digital subtraction angiography (DSA) as the gold standard. Methods: This retrospective study included 60 patients diagnosed with lower extremity arterial stenosis occlusion (LEASO) from October 2019 to July 2022. All patients underwent 3D CE-MRA and ultrasound microbubble angiography, collectively assessing 470 arterial segments. The diagnostic accuracy, sensitivity, and specificity of 3D CE-MRA, ultrasound microbubble angiography, and their combination were evaluated compared to DSA findings. Kappa statistics were used to analyze the consistency of combined diagnostic efficacy. Results: The cohort included subjects aged 56 to 85 years, with a mean age of 65.42 ± 12.65 years. The diagnostic accuracy of 3D CE-MRA was 91.70%, with sensitivity and specificity of 99.72% and 65.49%, respectively. Ultrasound microbubble angiography revealed an 87.66% accuracy with sensitivity and specificity of 99.13% and 56.35%, respectively. When combined, the diagnostic accuracy was improved to 96.17%, maintaining a sensitivity of 100%, although specificity decreased to 50.44%. The Youden index improved to 96.17%, and the Kappa value of 0.951 indicated excellent agreement, demonstrating superior performance over individual modalities. Conclusion: The combination of 3D CE-MRA and ultrasound microbubble angiography exhibits enhanced diagnostic precision for detecting and grading LEASO compared to either modality alone. Despite reduced specificity, the combined approach increases overall diagnostic efficacy, advocating its potential for more comprehensive clinical evaluations. Further studies are warranted to confirm these findings and assess their clinical implications.

Keywords: Lower extremity arterial stenosis, 3D contrast-enhanced magnetic resonance angiography, ultrasound microbubble angiography, digital subtraction angiography, diagnostic accuracy, vascular imaging

Introduction

Lower extremity atherosclerotic occlusive (LEASO) disease is a prevalent condition characterized by the narrowing or blockage of peripheral arteries, primarily in the legs. LEASO affects millions of people worldwide, particularly older adults and individuals with risk factors such as diabetes, hypertension, and smoking. It manifests in a range of symptoms, from intermittent claudication (pain during walking that resolves with rest) to critical limb ischemia (severe pain, ulcers, and gangrene), and is associated with an elevated risk of cardiovascular events and mortality, imposing a substantial socioeconomic burden due to disability, reduced quality of life, and increased healthcare costs [1-3]. Accurate and early diagnosis of LEASO is crucial for implementing timely therapeutic interventions to prevent progression, preserve limb function, and improve quality of life [4]. Digital Subtraction Angiography (DSA), traditionally regarded as the gold standard for vascular imaging due to its high spatial resolution [5], is invasive and associated with risks from contrast agents and radiation exposure. Additionally, its reliance on specialized equipment and trained personnel limits accessibility in resource-limited settings [6, 7]. Therefore, there is a pressing need for non-invasive imaging techniques that can effectively assess arterial occlusions and stenoses while minimizing patient risk and healthcare costs.

Advancements in imaging technology have introduced several non-invasive modalities, including 3D Contrast-Enhanced Magnetic Resonance Angiography (3D CE-MRA) [8] and ultrasound microbubble angiography, which hold significant promise for the evaluation of vascular conditions like LEASO [7, 9]. 3D CE-MRA utilizes gadolinium-based contrast agents to produce high-resolution vascular images non-invasively, offering an alternative to DSA without ionizing radiation, thereby improving patient safety. Despite these benefits, CE-MRA has limitations in specificity, particularly in grading arterial stenosis, as it primarily focuses on anatomical visualization rather than functional assessment. This limitation highlights the need for complementary approaches to fully assess the hemodynamic implications of stenoses, which is critical for comprehensive clinical management [10-12].

Ultrasound microbubble angiography, on the other hand, provides a functional perspective by assessing blood flow and microvascular perfusion. This technique uses microbubble contrast agents that reflect ultrasound waves, allowing real-time visualization of blood flow dynamics, which is particularly beneficial for detecting perfusion deficits associated with stenosis or occlusion, providing a functional dimension that anatomical imaging alone may overlook. Nevertheless, ultrasound is limited by its dependence on the operator's expertise and reduced efficacy in imaging highly calcified or deeply situated vessels [13, 14].

The integration of 3D CE-MRA with ultrasound microbubble angiography offers a complementary diagnostic approach, potentially enhancing accuracy by combining anatomical detail with hemodynamic data. While each modality individually contributes valuable insights into vascular status, their integration addresses the deficiencies inherent in using a single technique. The anatomical precision of CE-MRA, when supplemented with the functional data provided by ultrasound, can offer a more robust assessment framework, improving diagnostic confidence and accuracy in evaluating the severity and implications of LEASO [15-17].

Current literature suggests that combining imaging modalities may enhance diagnostic efficacy and improve patient outcomes across a spectrum of vascular diseases [18, 19]. However, studies specifically addressing the benefits of combining CE-MRA with ultrasound microbubble angiography in LEASO remain limited. This gap highlights the need for comprehensive studies to evaluate the performance of their combined diagnosis, comparing it with traditional standards and exploring its potential to alter therapeutic decision-making and clinical outcomes. This study aims to assess the diagnostic accuracy, sensitivity, and specificity of 3D CE-MRA combined with ultrasound microbubble angiography in the diagnosis of LEASO, using DSA as the reference standard.

Data and methods

Patient selection

The clinical data of 60 patients diagnosed with LEASO, who were admitted to the Second Affiliated Hospital of Qiqihar Medical University from October 2019 to July 2022, were retrospectively analyzed. All patients underwent both 3D CE-MRA and ultrasound microbubble angiography imaging, evaluating a total of 470 arterial segments. With DSA results as the gold standard, the accuracy, sensitivity, and specificity of the combined imaging modalities in determining the degree of lower limb arterial stenosis were analyzed. The quantitative parameter of 3D CE-MRA and ultrasound microbubble angiography can be found in Supplementary Material 1.

Inclusion criteria: 1) Patients aged between 56 and 85 years; 2) Presentation of early-stage symptoms, including lower limb pain, muscle swelling, occasional numbness during ambulation, and weak dorsalis pedis arterial pulsation, and in severe cases, intermittent claudication along with tissue gangrene or limb ischemia [20], requiring differentiation from LEASO; 3) Patients who underwent both 3D CE-MRA and ultrasound microbubble angiography. Exclusion criteria: 1) Patients who had undergone surgical treatments such as endovascular therapy, incision, thrombus extraction, or arterial bypass grafting; 2) Those with renal insufficiency, a history of contrast agent allergies, implanted cardiac pacemakers, or claustrophobia (**Figure 1**).

This study received approval from the Institutional Review Board and Ethics Committee of Qiqihar Medical University (approval no:

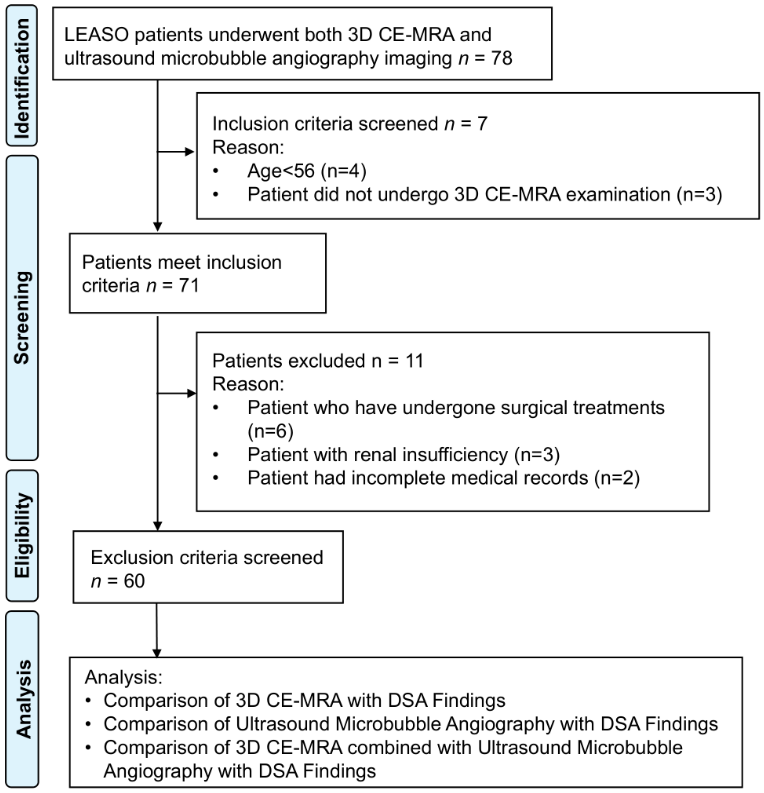

Figure 1. Study flow diagram.

2022-47). Given that the study utilized de-identified patient data exclusively, which presented no potential harm or impact on the patients, the requirement for informed consent was waived. This waiver was granted by the Institutional Review Board and Ethics Committee in compliance with the regulatory and ethical standards governing retrospective research studies.

Data extraction

3D CE-MRA: Imaging was conducted using a PHILIPS Ingenia 3.0T MR scanner with dedicated lower limb array coils. A 15 ml Gadobenate Dimeglumine injection was used as the contrast agent, administered rapidly via a bolus injection using the Spectris Solaris EP power injector. The 3.0T system seamlessly stitched three vessel segments together and combined them with original image analysis, minimizing the risk of suboptimal reconstructed image displays or ambiguous diagnoses (**Figure 2**).

DSA: DSA was performed using a PHILIPS Azurion 7M20 large C-arm digital subtraction X-ray machine, with multi-functional catheters from COOK company and a Markerplus high-pressure injector from the United States. Iodixanol was used as the contrast agent, administered at an injection rate of 3.0-5.0 ml/s. The Seldinger technique was used for femoral artery puncture, followed by routine (anterograde or retrograde) segmental angiography of the bilateral lower limb arteries (**Figure 3**).

Ultrasound microbubble angiography: The patient was immobilized in bed during the examination. Initial evaluation of bilateral lower extremity arterial blood flow was performed using color Doppler ultrasound to identify arterial stenosis or occlusion. Subsequently, a microbubble ultrasound contrast agent (SonoVue, Bracco Imaging, Milan, Italy) was administered intravenously. This agent produced microscopic air bubbles, which then entered the bloodstream. Subsequently, using an ultrasound probe (PHILIPS EPIQ 7C, Philips Healthcare, Best, Netherlands), the physician scanned the area of interest, emitting ultrasound waves to capture both arterial blood flow dynamics and assess the microbubble contrast agent. The reflected ultrasound waves enhanced arterial blood flow visualization, enabling the evaluation of perfusion and the identification of stenosis, occlusion, or thrombosis. Analysis of blood flow velocity and the distribution patterns of the microbubble contrast agent facilitated the diagnosis of atherosclerotic occlusion in the lower extremities (**Figure 4**).

Outcome measures

The lower limb arteries were divided into three major segments: Infra-genicular arterial segments (anterior tibial artery, popliteal-trunk artery, peroneal artery, and posterior tibial artery), Femoral-popliteal arterial segments (femoral artery, superficial femoral artery, deep

Figure 2. Example of 3D CE-MRA images showing the lower limb vasculature. A: Normal. B: Mild stenosis. C: Moderate stenosis. D: Severe stenosis. E: Complete occlusion. 3D CE-MRA: 3D contrast-enhanced magnetic resonance angiography.

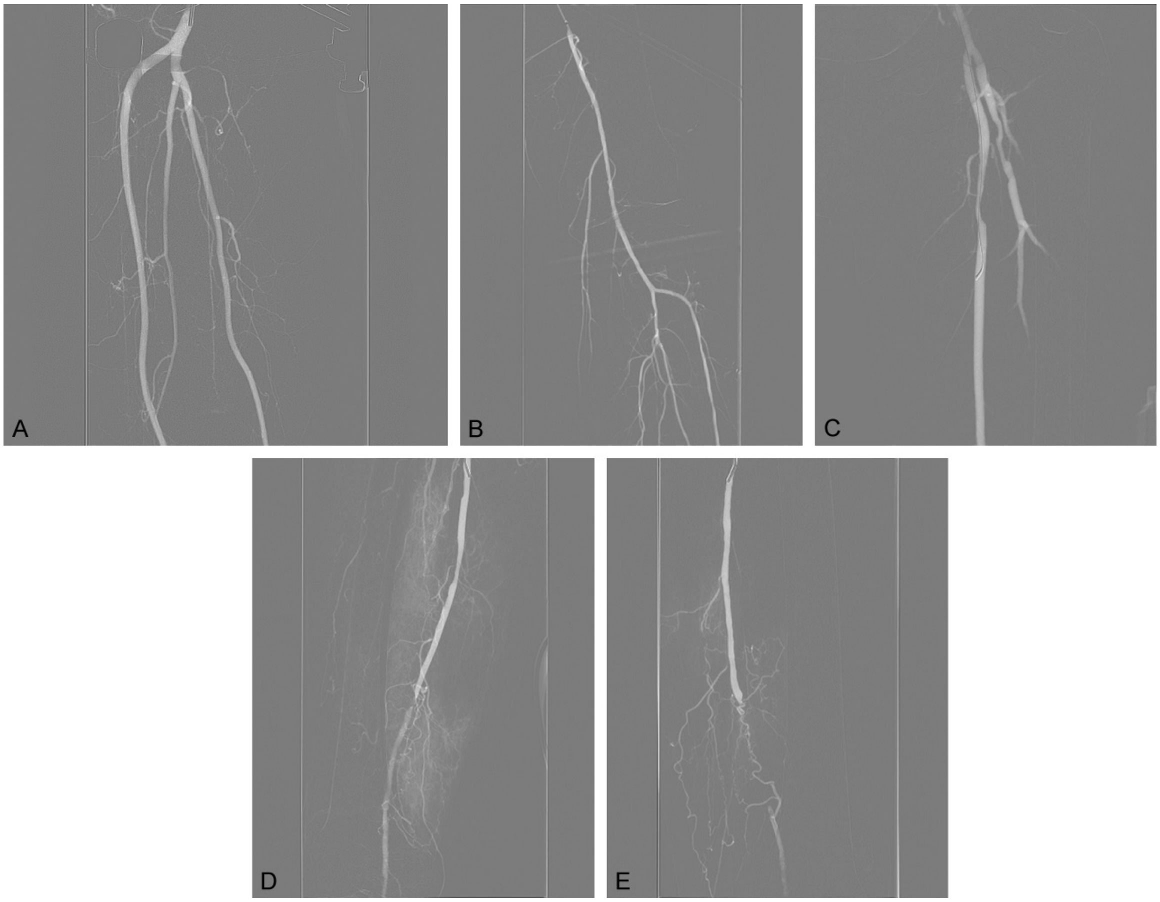

Figure 3. Example of DSA images showing the lower limb vasculature. A: Normal lower extremity arteries. B: Mild stenosis. C: Moderate stenosis. D: Severe stenosis. E: Occlusion. DSA: digital subtraction angiography.

femoral artery, and popliteal artery), Iliac arterial segments (common iliac artery, external iliac artery, and internal iliac artery). These segments were further sub-divided into 22 minor segments according to the grading method for peripheral vascular occlusive disease. The degree of stenosis in the lower limb arteries was categorized into five levels: occlusion (100%), severe stenosis (75%-99%), moderate stenosis (50%-74%), mild stenosis (1%-49%), and normal (no stenosis) [21]. In cases where multiple stenoses were present in the diseased vessel, the highest level of stenosis was classified.

The degree of arterial stenosis and occlusion, as obtained from 3D DCE MRA, DSA, and ultrasound microbubble angiography, was assessed by MR physicians, DSA assessed, and ultrasound microbubble angiography physicians, each independently, without prior comparison of the images. Specific methods for measuring vascular stenosis: 1. Measure the diameter at the narrowest part of the corresponding diseased segment (diameter of the most stenotic artery, Ds); 2. Measure the diameter approximately 1-3 cm away from Ds (diameter of the normal artery, Dn); 3. Calculate the luminal stenosis rate using the formula: (Dn - Ds)/Dn × 100% [22]. The degree of vascular stenosis, as measured by both physicians, was recorded, and the average value was taken. The stenosed segments were also marked. If there were significant discrepancies between the measurements of the two physicians, a third physician remeasured the segment. Grade I: Mild stenosis; Grade II: Moderate stenosis; Grade III: Severe stenosis; Grade IV: Occlusion.

Statistical analysis

Statistical analysis was conducted using SPSS version 26.0 (IBM Corp., Armonk, NY, USA). Count data were expressed as [n (%)] and com-

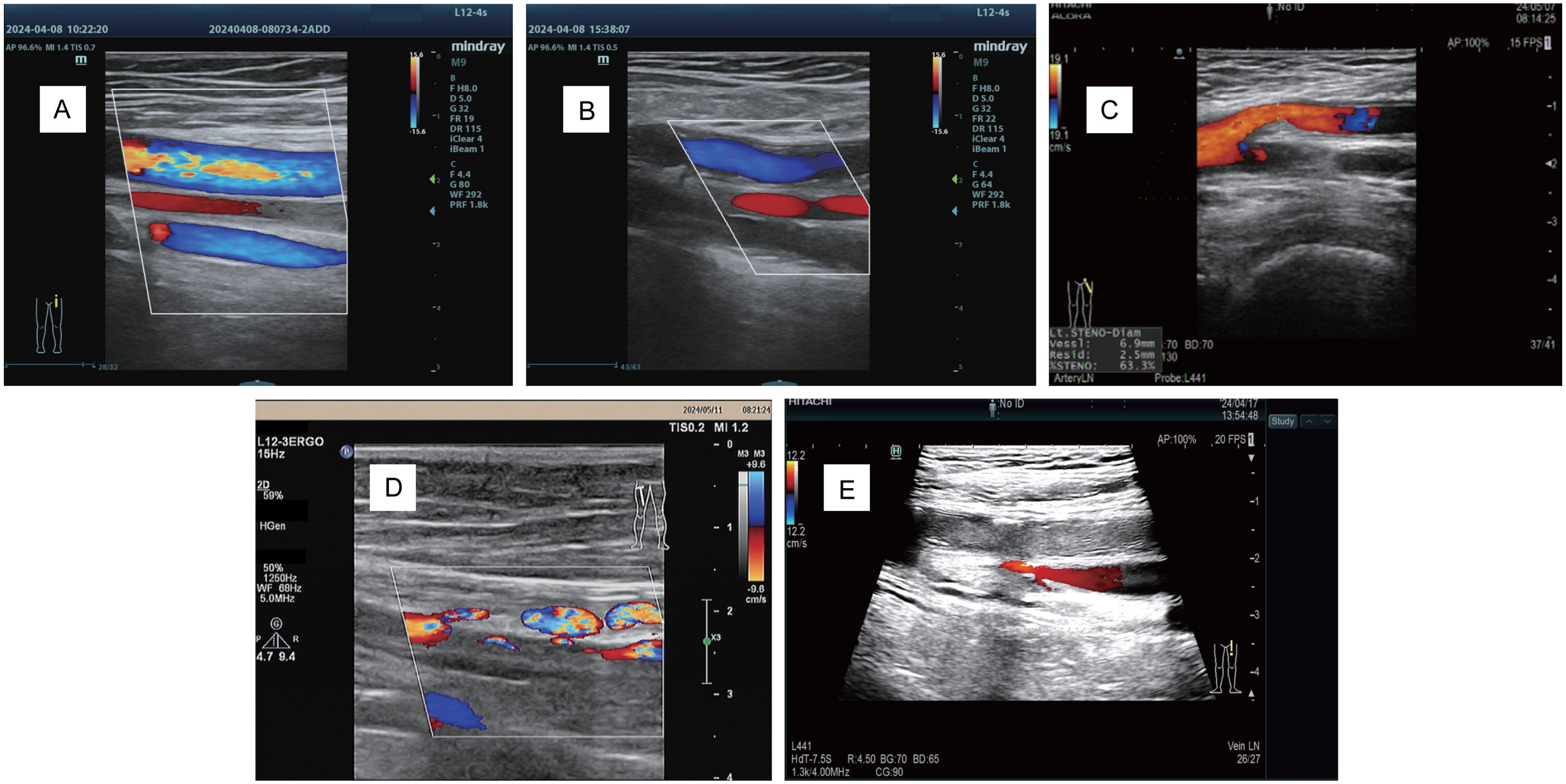

Figure 4. Example of ultrasound microbubble angiography images showing the lower limb vasculature. A: Normal lower extremity arteries. B: Mild stenosis. C: Moderate stenosis. D: Severe stenosis. E: Occlusion.

Table 1. Baseline characteristics of included cases

Parameters	Baseline data (n = 60)
Age (mean ± SD)	65.42 ± 12.65 years
Gender (Male/Female)	36 (60.00%)/24 (40.00%)
BMI (kg/m^2)	21.32 ± 3.32
Smoking history [n/(%)]	22 (36.67%)
Hypertension [n/(%)]	30 (50.00%)
Hyperlipidemia [n/(%)]	25 (41.67%)
Diabetes mellitus [n/(%)]	18 (30.00%)
Relevant adverse symptoms	
Lower limb pain	58 (96.67%)
Swelling of lower limb muscles	45 (75.00%)
Occasional numbness during ambulation	30 (50.00%)
Weak dorsalis pedis arterial pulsation	50 (83.33%)
Intermittent claudication along with manifestations of tissue gangrene	15 (25.00%)
Limb ischemia	12 (20.00%)

BMI: Body Mass Index.

pared between groups using the χ^2 test. Continuous variables were expressed as mean ± standard deviation (SD) and analyzed using Student's t-test or ANOVA, as appropriate. Kappa statistics were used to assess the agreement between the diagnostic modalities, with Kappa ≥ 0.75 indicating excellent agreement, 0.4 ≤ Kappa < 0.75 indicating fair to good agreement, and Kappa < 0.4 indicating poor agreement. Diagnostic performance measures (accuracy, sensitivity, and specificity) were calculated using DSA results as the reference standard. The formulas for these measures are as follows: Diagnostic accuracy: number of cases where 3D CE-MRA or ultrasound microbubble angiography results agree with DSA/total number of cases × 100%; Arterial stenosis grade 0 was considered negative (-) and grades I-IV were considered positive (+). Accuracy: (True Positive + True Negative)/Total Cases × 100%; Sensitivity: True Positive/(True Positive + False Negative) × 100%; Specificity: True Negative/(True Negative + False Positive) × 100%. Confidence intervals (CIs) were calculated for each measure, and a p-value < 0.05 was considered statistically significant.

Results

Baseline characteristics of participants

The mean age of the participants was 65.42 ± 12.65 years (n = 60) (**Table 1**). The cohort comprised predominantly males (36, 60.00%) compared to females (24, 40.00%). The average body mass index (BMI) was 21.32 ± 3.32 kg/m^2. Smoking history was reported by 22 participants (36.67%), while hypertension affected 30 participants (50.00%), hyperlipidemia was observed in 25 participants (41.67%), and diabetes mellitus was present in 18 participants (30.00%). Regarding relevant symptoms, lower limb pain was prevalent among 58 participants (96.67%), swelling of lower limb muscles was noted in 45 participants (75.00%), and occasional numbness during ambulation was observed in 30 participants (50.00%). A weak dorsalis pedis arterial pulsation was detected in 50 participants (83.33%), intermittent claudication accompanied with manifestations of tissue gangrene was observed in 15 participants (25.00%), and limb ischemia was recorded in 12 participants (20.00%).

Comparison of 3D CE-MRA with DSA findings

The comparison of 3D CE-MRA with DSA findings for LEASO grading revealed distinct diagnostic accuracy across different grades. For 3D CE-MRA (**Table 2**), most cases were accurately diagnosed, particularly for normal cases (74/81, 91.36%) and Grade IV lesions (48/54, 88.89%). There were some discrepancies in the lower grades, with 88 correct identifications out of 95 cases (92.63%) in Grade I and 106 correct identifications out of 115 cases (92.17%) in Grade II. Grade III lesions were correctly identified in 115 out of 125 cases (92.00%).

Table 2. 3D CE-MRA versus DSA for LEASO diagnosis and grading

3D CE-MRA	The results of DSA					Total
	Normal	Grade I	Grade II	Grade III	Grade IV	
Normal	74	1	0	0	0	75
Grade I	7	88	3	0	0	98
Grade II	0	6	106	6	0	118
Grade III	0	0	6	115	6	127
Grade IV	0	0	0	4	48	52
Total	81	95	115	125	54	470

3D CE-MRA: 3D contrast-enhanced magnetic resonance angiography; DSA: digital subtraction angiography; LEASO: lower extremity arterial stenosis occlusion.

Table 3. Ultrasound microbubble angiography versus DSA for LEASO diagnosis and grading

Ultrasound microbubble angiography	The results of DSA					Total
	Normal	Grade I	Grade II	Grade III	Grade IV	
Normal	71	3	0	0	0	74
Grade I	10	84	7	0	0	101
Grade II	0	8	102	8	0	118
Grade III	0	0	6	110	9	125
Grade IV	0	0	0	7	45	52
Total	81	95	115	125	54	470

DSA: digital subtraction angiography; LEASO: lower extremity arterial stenosis occlusion.

Table 4. Combined modality versus DSA for LEASO diagnosis and grading

3D CE-MRA combined with ultrasound microbubble imaging	The results of DSA					Total
	Normal	Grade I	Grade II	Grade III	Grade IV	
Normal	79	0	0	0	0	79
Grade I	2	91	0	0	0	93
Grade II	0	4	112	6	0	122
Grade III	0	0	3	119	3	125
Grade IV	0	0	0	0	51	51
Total	81	95	115	125	54	470

3D CE-MRA: 3D contrast-enhanced magnetic resonance angiography; DSA: digital subtraction angiography; LEASO: lower extremity arterial stenosis occlusion.

Comparison of ultrasound microbubble angiography with DSA findings

For ultrasound microbubble angiography (**Table 3**), the diagnostic performance was similar to 3D CE-MRA but slightly less accurate. Normal cases were accurately diagnosed in 71 out of 81 cases (87.65%), while Grade IV lesions were identified correctly in 45 out of 54 cases (83.33%). Grade I lesions were correctly identified in 84 out of 95 cases (88.42%), and Grade II lesions were correctly identified in 102 out of 115 cases (88.70%). Grade III lesions were correctly identified in 110 out of 125 cases (88.00%).

Comparison of 3D CE-MRA combined with ultrasound microbubble angiography with DSA findings

When combining 3D CE-MRA with ultrasound microbubble angiography (**Table 4**), the diagnostic accuracy further improved. Normal cases were accurately diagnosed in 79 out of 81 cases (97.53%), and Grade IV lesions were identified correctly in 51 out of 54 cases (94.44%). Grade I lesions were identified correctly in 91 out of 95 cases (95.79%), Grade II lesions were identified in 112 out of 115 cases (97.39%), and Grade III lesions were correctly identified in 119 out of 125 cases (95.20%).

Table 5. Multivariate analysis of 3D CE-MRA and ultrasound microbubble angiography

Parameters	Coefficient	Std_Error	t_value	*P*_value
3D-CE-MRA	0.664	0.034	19.282	< 0.001
Ultrasound microbubble angiography	0.341	0.035	9.887	< 0.001

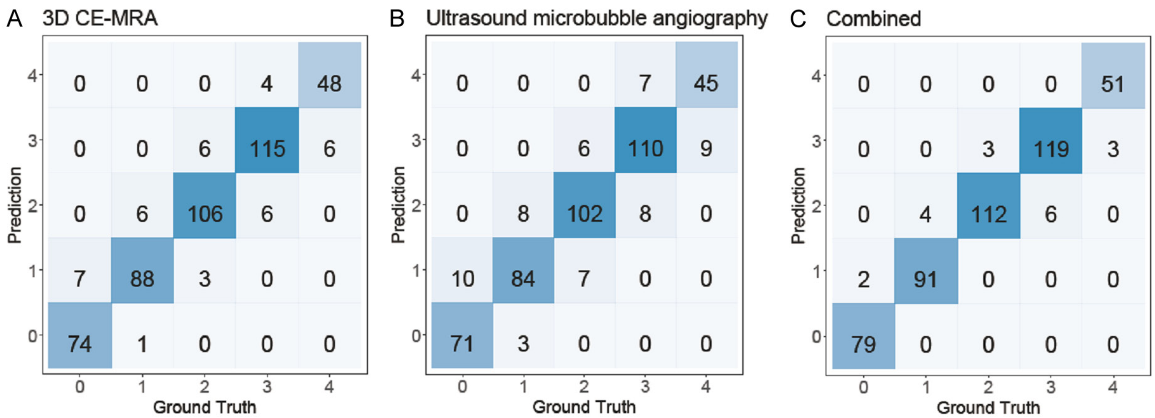

Figure 5. Summary confusion matrix comparing diagnostic performance of 3D CE-MRA, ultrasound microbubble angiography, and their combination for LEASO. A: 3D CE-MRA. B: Ultrasound microbubble angiography. C: 3D CE-MRA combined with ultrasound microbubble angiography. 3D CE-MRA: 3D contrast-enhanced magnetic resonance angiography; LEASO: lower extremity arterial stenosis occlusion.

Table 6. Diagnostic efficacy of 3D CE-MRA, ultrasound microbubble angiography, and their combination for LEASO

Method	Diagnostic efficiency						
	Accuracy (%)	Sensitivity (%)	Youden index (%)	Specificity (%)	Kappa	95% CI	P
3D-CE-MRA	91.70%	99.72%	91.42%	65.49%	0.894	0.888-0.940	< 0.001
Ultrasound microbubble angiography	87.66%	99.13%	86.79%	56.35%	0.843	0.843-0.905	< 0.001
3D-CE-MRA combined with ultrasound microbubble angiography	96.17%	100%	93.17%	50.44%	0.951	0.940-0.977	< 0.001

3D CE-MRA: 3D contrast-enhanced magnetic resonance angiography; LEASO: lower extremity arterial stenosis occlusion.

Multivariate analysis of 3D CE-MRA and ultrasound microbubble angiography

In the multivariate analysis comparing 3D-CE-MRA and ultrasound microbubble angiography (**Table 5**), both imaging techniques were significantly associated with the outcome parameters (3D-CE-MRA: Coefficient = 0.664, Standard Error = 0.034, t-value = 19.282, P < 0.001; Ultrasound microbubble angiography: Coefficient = 0.341, Standard Error = 0.035, t-value = 9.887, P < 0.001). 3D-CE-MRA exhibited a stronger association compared to ultrasound microbubble angiography, indicating its superior performance or impact on the evaluated outcomes. The significant coefficients for both methods underscore their importance in enhancing diagnostic accuracy and clinical decision-making processes.

Diagnostic efficacy of D-CE-MRA, ultrasound microbubble angiography, and their combination in LEASO

A summary confusion matrix (**Figure 5**) was presented comparing the diagnostic performance of each method for LEASO, showing the number of true positive, false positive, true negative, and false negative predictions made by each method. The combined examination yielded the highest accuracy, followed by 3D CE-MRA, and then ultrasound microbubble angiography. In the evaluation of diagnostic efficiency at different levels (**Tables 6** and **7**), the accuracy, sensitivity, Youden index, specificity, Kappa coefficient, and their 95% confidence interval (CI) were reported for each method. All three methods showed high diagnostic efficiency, with significant differences

Table 7. Diagnostic efficiency of each method for various grades of LEASO

Parameters	Method	Accuracy	Sensitivity	Specificity	PPV	NPV
Normal	3D-CE-MRA	0.917	0.913	0.997	0.986	0.982
Grade I	3D-CE-MRA	0.917	0.926	0.973	0.897	0.981
Grade II	3D-CE-MRA	0.917	0.921	0.966	0.898	0.974
Grade III	3D-CE-MRA	0.917	0.920	0.965	0.905	0.970
Grade IV	3D-CE-MRA	0.917	0.888	0.990	0.923	0.985
Normal	Ultrasound	0.876	0.876	0.992	0.959	0.974
Grade I	Ultrasound	0.876	0.884	0.954	0.831	0.970
Grade II	Ultrasound	0.876	0.886	0.954	0.864	0.963
Grade III	Ultrasound	0.876	0.880	0.956	0.880	0.956
Grade IV	Ultrasound	0.876	0.833	0.983	0.865	0.978
Normal	Combined	0.961	0.975	1.000	1.000	0.994
Grade I	Combined	0.961	0.957	0.994	0.978	0.989
Grade II	Combined	0.961	0.973	0.971	0.918	0.991
Grade III	Combined	0.961	0.952	0.982	0.952	0.982
Grade IV	Combined	0.961	0.944	1.000	1.000	0.992

3D CE-MRA: 3D contrast-enhanced magnetic resonance angiography; LEASO: lower extremity arterial stenosis occlusion; PPV: positive predictive value; NPV: negative predictive value.

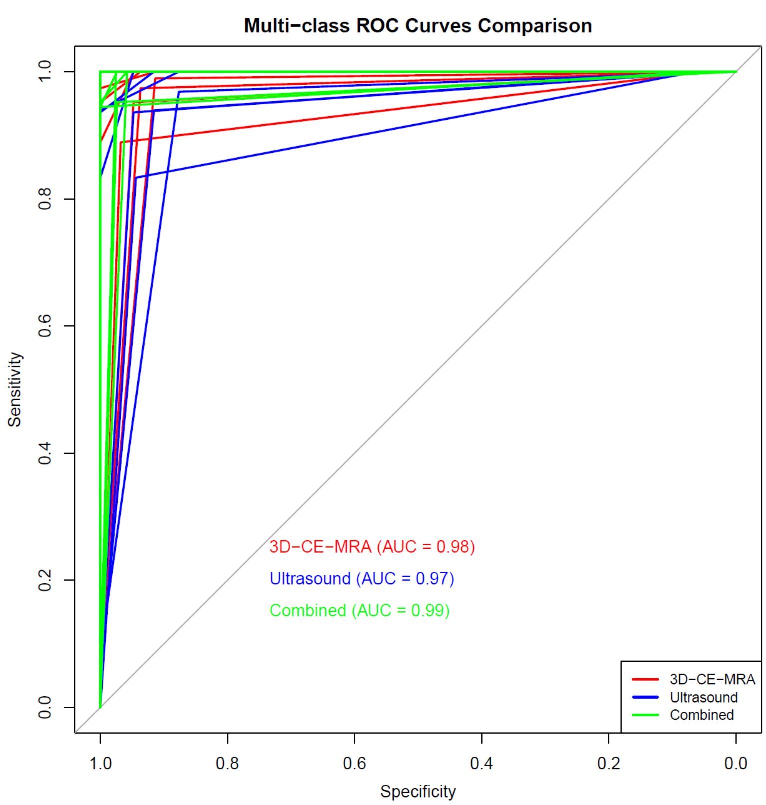

Figure 6. ROC curves for 3D CE-MRA, ultrasound microbubble angiography, and their combination for diagnosing LEASO. ROC: Receiver Operating Characteristic.

between them. 3D CE-MRA had an accuracy of 91.70%, sensitivity of 99.72%, and specificity of 65.49%. Ultrasound microbubble angiography had slightly lower accuracy at 87.66%, but still maintained high sensitivity at 99.13% and specificity at 56.35%. The combined method resulted in the highest accuracy of 96.17%, perfect sensitivity of 100%, and specificity of 50.44%. In summary, the combination of 3D CE-MRA and ultrasound microbubble angiography demonstrated superior diagnostic performance compared to either method alone, suggesting that this approach may be more effective in detecting LEASO (**Figure 6**).

Discussion

In this study, we explored the diagnostic efficacy of combining 3D CE-MRA with ultrasound microbubble angiography for detecting LEASO. Our findings indicated that the combined diagnostic approach offered superior accuracy, sensitivity, and specificity compared to either imaging modality used independently.

These results underscore the potential advantages of integrating multiple imaging modalities to enhance diagnostic accuracy in LEASO evaluation.

The success of combining 3D CE-MRA and ultrasound microbubble angiography can be attributed to the complementary strengths of both techniques. 3D CE-MRA provides detailed anatomical imaging and excellent visualization of the vasculature, including calcified regions, without the need for ionizing radiation, a significant advantage over traditional DSA. Previous studies have demonstrated the excellent sensitivity of 3D CE-MRA, which is consistent with our study results (99.72%) [23, 24]. However, one limitation of MRA is its lower specificity, particularly in distinguishing between various stages of stenosis, due to the reliance on gadolinium-based contrast agents, which may not offer sufficient delineation of arterial wall characteristics [25-27].

Ultrasound microbubble angiography, on the other hand, enhances diagnostic capability by incorporating real-time hemodynamic information. The use of microbubble contrast agents allows for the differentiation between blood flow-related changes and static anatomical formations, which is particularly useful in assessing stenoses and occlusions. The dynamic nature of ultrasound allows for the direct assessment of blood flow velocity and can discern perfusion patterns associated with varying degrees of arterial occlusion. However, the spatial resolution is inherently limited by the ultrasound's ability to penetrate deeply calcified or densely occluded vessels [28, 29].

The integration of these modalities leverages their complementary attributes. 3D CE-MRA's detailed structural imaging enhances spatial resolution and anatomical comprehension, while ultrasound microbubble angiography contributes dynamic, functional insights into blood flow patterns [15, 26]. This combination likely results in improved detection capabilities for varying degrees of stenosis and occlusion, as evidenced by higher Kappa values and Youden indices reported in our study. The seamless integration of morphological and functional data proves crucial in resolving diagnostic ambiguities that may arise when relying on a singular imaging technique.

The enhanced sensitivity and specificity observed in our study are significant for clinical practice. In particular, the increased sensitivity of the combined approach ensures fewer false negatives, an essential factor in preventing the progression and complications of undiagnosed LEASO. The ability to accurately detect even minor stenotic changes (as indicated by increased accuracy in lower-grade lesions) is pivotal in early intervention and management strategies, potentially minimizing therapy invasiveness and improving patient prognoses [30].

Our study also highlights the distinct improvement in diagnosis accuracy when both modalities are combined, reaching 96.17%. These findings suggest that this combined approach may be particularly useful in complex cases where individual modalities yield ambiguous results. For instance, if ultrasound microbubble angiography indicates potential stenosis but lacks high spatial resolution, the 3D anatomical context provided by CE-MRA becomes invaluable in confirming the diagnosis, quantifying stenosis, and planning therapeutic interventions [10, 31].

Furthermore, the difference in specificity between the two modalities reflects the inherent trade-offs in imaging. While 3D CE-MRA offers a detailed anatomical overview, it may identify benign anatomic variants as pathological [10]. In contrast, ultrasound microbubble angiography, though less specific in isolation, compensates by providing functional data that can refute these false positives [32]. The observed decrease in specificity when both tests are combined reflects this trade-off, but it is mitigated by the significant increase in overall diagnostic confidence, as demonstrated by the improved Kappa value.

Nonetheless, several challenges and limitations need to be addressed in future research. The most notable limitation of this dual-imaging approach is its increased cost and logistical demands. Conducting both imaging modalities may not be feasible in all clinical settings due to equipment availability, required expertise, and patient-related factors (such as contraindications to gadolinium use or ultrasound accessibility issues). Therefore, the role of the combined approach should be carefully considered in terms of patient selection criteria and cost-effectiveness in clinical practice. Moreover, while the diagnostic accuracy of the dual approach is promising, longitudinal studies are needed to assess its impact on long-term patient outcomes. It remains unclear how enhanced diagnostic precision translates into clinical benefits, such as reduced mortality or improved quality of life. Larger, multicentric trials are essential to validate these findings across diverse populations and establish firm guidelines for integrating this approach into clinical workflows.

This study has several limitations that should be acknowledged. First, the retrospective design may introduce selection bias, as we relied on previously collected data that may not fully represent a broader range of clinical scenarios. While the sample size is adequate for preliminary analysis, it remains relatively small, limiting the generalizability of our findings to diverse populations. Another significant limitation is the lack of additional diagnostic indices beyond accuracy, sensitivity, and specificity. Due to the retrospective nature of the study, we did not have access to other potential metrics that could provide a more comprehensive evaluation of the combined imaging approach. This limitation restricts the depth of our analysis and the generalizability of our findings. Future prospective studies with larger and more diverse cohorts should aim to incorporate a broader range of diagnostic metrics to better assess the clinical utility and impact of the combined 3D CE-MRA and ultrasound microbubble angiography approach. Additionally, while the combined imaging approach demonstrated improved diagnostic accuracy, its implementation requires specialized equipment and expertise, which may not be accessible in all clinical settings. Finally, the reliance on DSA as the gold standard, despite its own limitations, could potentially influence comparative efficacy assessments. Future studies should consider prospective designs with larger, more diverse cohorts and evaluate cost-effectiveness of the combined approach to better understand its impact on clinical outcomes and healthcare systems.

Conclusion

In conclusion, our study indicates that the combination of 3D CE-MRA and ultrasound microbubble angiography significantly enhances the diagnostic accuracy for LEASO. This integrated approach should be considered for inclusion in diagnostic algorithms, particularly for ambiguous cases or when initial imaging results are inconclusive. Future work should focus on technological advancements, cost-benefit analyses, and outcome studies to refine its application and improve patient care. Such integration of multimodal imaging holds great promise in vascular diagnostics, underscoring the potential of inter-disciplinary approaches to solving complex clinical challenges.

Acknowledgements

This research was supported by the Science and Technology Programs of Heilongjiang Provincial Health and Wellness Commission (20220909010616).

Disclosure of conflict of interest

None.

Address correspondence to: Junzhi Sang, The Medical Imaging Center, The Second Affiliated Hospital of Qiqihar Medical University, Zhonghuaxi Road 37, Qiqihar 161006, Heilongjiang, China. E-mail: SangJz.BMedMR@qmu.edu.cn

References

[1] Wang QH, Tang C, Wang YM, Cai J, Wang W, Ran F and Qiao T. Correlation and predictive value analysis of iliac artery calcification score and restenosis of lower extremity arteries after drug-coated balloon combined with stent implantation in patients with lower extremity atherosclerotic occlusive disease. Zhonghua Yi Xue Za Zhi 2024; 104: 3520-3527.

[2] Moaaz M and Lotfy H. Changes and significance of T helper-9 cells and interleukin-9 in patients with atherosclerotic chronic lower limb ischemia: effect on IL-17 release. Vascular 2020; 28: 378-389.

[3] He Y, Wang S, Deng J, Pu Q, Chen H and Huang L. Chlamydia psittaci pneumonia complicated with lower extremity atherosclerotic occlusive disease. Infect Drug Resist 2023; 16: 2141-2145.

[4] Xiao D and Song J. Clinical efficacy of interventional therapy on lower extremity arteriosclerosis obliterans and prognostic factors. Comput Math Methods Med 2022; 2022: 9190292.

[5] Wang J, Fu D, Tang C, Shu G, Zhang X, Zhang X, Pan J and Sun SK. Bismuth chelate-mediated digital subtraction angiography. Adv Healthc Mater 2024; 13: e2401653.

[6] Fridh EB, Ludwigs K, Svalkvist A, Andersson M, Nordanstig J, Falkenberg M and Johnsson ÅA. Comparison of magnetic resonance angiography and digital subtraction angiography for the assessment of infrapopliteal arterial occlusive lesions, based on the TASC II classification criteria. Diagnostics (Basel) 2020; 10: 892.
[7] Posa A, Tanzilli A, Barbieri P, Steri L, Arbia F, Mazza G, Longo V and Iezzi R. Digital subtraction angiography (DSA) technical and diagnostic aspects in the study of lower limb arteries. Radiation 2022; 2: 376-386.
[8] Zhao DL, Li RY, Li C, Chen XH, Yu JW, Zhang Y and Ju S. Assessment of the degree of arterial stenosis in intracranial atherosclerosis using 3D high-resolution MRI: comparison with time-of-flight MRA, contrast-enhanced MRA, and DSA. Clin Radiol 2023; 78: e63-e70.
[9] Knobloch G, Lauff MT, Hanke M, Schwenke C, Hamm B and Wagner M. Non-contrast-enhanced MR-angiography (MRA) of lower extremity peripheral arterial disease at 3 tesla: examination time and diagnostic performance of 2D quiescent-interval single-shot MRA vs. 3D fast spin-Echo MRA. Magn Reson Imaging 2021; 76: 17-25.
[10] Bergmann LL and François CJ. Current imaging approaches and challenges in the assessment of peripheral artery disease. Vessel Based Imaging Techniques: Diagnosis, Treatment, and Prevention 2020; 147-157.
[11] Hosadurg N and Kramer CM. Magnetic resonance imaging techniques in peripheral arterial disease. Adv Wound Care (New Rochelle) 2023; 12: 611-625.
[12] Tatli S and Yucel EK. MRA of the aorta and peripheral arteries: vertragliche schuldverhltnisse. Cardiovascular Magnetic Resonance Imaging 2019; 381-405.
[13] Harmon JN, Khaing ZZ, Hyde JE, Hofstetter CP, Tremblay-Darveau C and Bruce MF. Quantitative tissue perfusion imaging using nonlinear ultrasound localization microscopy. Sci Rep 2022; 12: 21943.
[14] Brahmandam A, Chan SM, Dardik A, Nassiri N and Aboian E. A narrative review on the application of high-intensity focused ultrasound for the treatment of occlusive and thrombotic arterial disease. JVS Vasc Sci 2022; 3: 292-305.
[15] David E, Grazhdani H, Aliotta L, Gavazzi LM, Foti PV, Palmucci S, Inì C, Tiralongo F, Castiglione D, Renda M, Pacini P, Di Bella C, Solito C, Gigli S, Fazio A, Bella R, Basile A and Cantisani V. Imaging of carotid stenosis: where are we standing? Comparison of multiparametric ultrasound, CT angiography, and MRI angiography, with recent developments. Diagnostics (Basel) 2024; 14: 1708.
[16] Saloner D. For evaluating hemodynamics. Vessel Based Imaging Techniques: Diagnosis, Treatment, and Prevention 2019; 331.
[17] Abbasi MA, Pathrose A, Serhal AM and Carr J. Imaging approaches for aortic disease. Vessel Based Imaging Techniques: Diagnosis, Treatment, and Prevention 2020; 173-208.
[18] Duering M, Biessels GJ, Brodtmann A, Chen C, Cordonnier C, de Leeuw FE, Debette S, Frayne R, Jouvent E, Rost NS, Ter Telgte A, Al-Shahi Salman R, Backes WH, Bae HJ, Brown R, Chabriat H, De Luca A, deCarli C, Dewenter A, Doubal FN, Ewers M, Field TS, Ganesh A, Greenberg S, Helmer KG, Hilal S, Jochems ACC, Jokinen H, Kuijf H, Lam BYK, Lebenberg J, MacIntosh BJ, Maillard P, Mok VCT, Pantoni L, Rudilosso S, Satizabal CL, Schirmer MD, Schmidt R, Smith C, Staals J, Thrippleton MJ, van Veluw SJ, Vemuri P, Wang Y, Werring D, Zedde M, Akinyemi RO, Del Brutto OH, Markus HS, Zhu YC, Smith EE, Dichgans M and Wardlaw JM. Neuroimaging standards for research into small vessel disease-advances since 2013. Lancet Neurol 2023; 22: 602-618.
[19] Kamenský V, Rogalewicz V, Gajdoš O, Donin G, Mašková B, Holá M and Tichopád A. Cost-effectiveness of diagnostic imaging modalities in symptomatic patients with lower limb peripheral arterial disease: discrete event simulation model. Front Public Health 2024; 12: 1367447.
[20] Chou TH and Stacy MR. Clinical applications for radiotracer imaging of lower extremity peripheral arterial disease and critical limb ischemia. Mol Imaging Biol 2020; 22: 245-255.
[21] Vlachopoulos C, Georgakopoulos C, Koutagiar I and Tousoulis D. Diagnostic modalities in peripheral artery disease. Curr Opin Pharmacol 2018; 39: 68-76.
[22] Kang T, Mukherjee D and Ryu J. Hemodynamic flow characteristics at stenosed artery: numerical analysis of three-dimensional patient-specific aortic-cerebral vasculature exposed to progressive carotid stenosis. Physics of Fluids 2022; 34.
[23] Pennig L, Wagner A, Weiss K, Lennartz S, Huntgeburth M, Hickethier T, Maintz D, Naehle CP, Bunck AC and Doerner J. Comparison of a novel compressed SENSE accelerated 3D modified relaxation-enhanced angiography without contrast and triggering with CE-MRA in imaging of the thoracic aorta. Int J Cardiovasc Imaging 2021; 37: 315-329.
[24] Calloni SF, Perrotta M, Roveri L, Panni P, Del Poggio A, Vezzulli PQ, Filippi M, Falini A and Anzalone N. The role of CE-MRA of the supraortic vessels in the detection of associated intracranial pathology. Neurol Sci 2021; 42: 5131-5137.

[25] Shwaiki O, Rashwan B, Fink MA, Kirksey L, Gadani S, Karuppasamy K, Melzig C, Thompson D, D'Amico G, Rengier F and Partovi S. Lower extremity CT angiography in peripheral arterial disease: from the established approach to evolving technical developments. Int J Cardiovasc Imaging 2021; 37: 3101-3114.
[26] David E, Martinelli O, Pacini P, Di Serafino M, Huang P, Dolcetti V, Del Gaudio G, Barr RG, Renda M, Lucarelli GT, Di Marzo L, Clevert DA, Solito C, Di Bella C and Cantisani V. New technologies in the assessment of carotid stenosis: beyond the color-Doppler ultrasound-high frame rate vector-flow and 3D arterial analysis ultrasound. Diagnostics (Basel) 2023; 13: 1478.
[27] Neumann S, Milano EG, Bucciarelli-Ducci C and Biglino G. Imaging the carotid atherosclerotic plaque. Vasc Biol 2019; 1: H53-H58.
[28] Gharat SK, Godiyal SC, Malusare PP, Jadhav KR and Kadam VJ. Microbubbles contrast agents: general overview as diagnostics and therapeutic agent. Curr Drug Targets 2022; 23: 960-977.
[29] Halfmann MC, Bockius S, Emrich T, Hell M, Schoepf UJ, Laux GS, Kavermann L, Graafen D, Gori T, Yang Y, Kloeckner R, Maurovich-Horvat P, Ricke J, Müller L, Varga-Szemes A and Fink N. Ultrahigh-spatial-resolution photon-counting detector CT angiography of coronary artery disease for stenosis assessment. Radiology 2024; 310: e231956.
[30] Zheng H, Calligaro KD, Jang J, Tyagi S, Madden N, Troutman DA and Dougherty MJ. Duplex ultrasound for diagnosis of failing stents placed for lower extremity arterial occlusive disease. Ann Vasc Surg 2020; 63: 269-274.
[31] Ironi G, Brembilla G, Benedetti G and De Cobelli F. Anatomical overview and imaging of the aorta and visceral arteries. Visceral Vessels and Aortic Repair: Challenges and Difficult Cases 2019; 3-17.
[32] Nederhoed JH, Tjaberinga M, Otten RHJ, Evers JM, Musters RJP, Wisselink W and Yeung KK. Therapeutic use of microbubbles and ultrasound in acute peripheral arterial thrombosis: a systematic review. Ultrasound Med Biol 2021; 47: 2821-2838.